Final Draft
of the original manuscript:

Amancio-Filho, S.T.; Roeder, J.; Pereira Nunes, S.; dos Santos, J.F.;
Beckmann, F.:

Thermal degradation of polyetherimide joined by friction riveting (FricRiveting). Part I: Influence of rotation speed

In: Polymer Degradation and Stability (2008) Elsevier

DOI: 10.1016/j.polymdegradstab.2008.05.019

Thermal degradation of polyetherimide joined by friction riveting (FricRiveting). Part I: influence of rotation speed

S.T. Amancio-Filho [a,*] , J. Roeder [b], S. P. Nunes [b], J.F. dos Santos [a], F. Beckmann [c]

[a] *GKSS Forschungszentrum Geesthacht GmbH, Institute of Materials Research, Materials Mechanics, Solid State Joining Processes (WMP) Max-Planck-Str. 1, D-21502 Geesthacht, Germany.* Tel. +49 4152 87 2066; fax: +49 4152 87 2033. E-mail address: sergio.amancio@gkss.de

[b] *GKSS Forschungszentrum Geesthacht GmbH, Institute of Polymer Research, Max-Planck-Str. 1, D-21502 Geesthacht, Germany.*

[c] *GKSS Forschungszentrum Geesthacht GmbH, Institute of Materials Research, Materials Physics (WFN-DESY) Max-Planck-Str. 1, D-21502 Geesthacht, Germany*

Abstract

In this work the thermal degradation of polyetherimides joined by friction riveting (FricRiveting) [1] was investigated for variable rotation speeds. The rotation speed is an important variable to be understood in order to predict thermal degradation during this process. Investigated rotation speeds in the range of 1570-2199 rad/s resulted in high process temperatures (350-475 ^{o}C) and heating rates (up to 2 ^{o}C/100 rad.s^{-1}), but only small heating times (< 3s). Thermal degradation was evaluated by gel permeation chromatography, Fourier transform infrared spectroscopy and X-ray computer microtomography. Results indicated that thermal degradation in the PEI polymer was mainly due to chain scission. Moreover, the small level of thermal degraded material (average drops of 10% in molecular weight) showed only a minor dependence with rotation speed. Although high peak temperatures and heating rates were

present, the restricted variation and average values of heating time were insufficient to cause strong thermal changes in the joints of the studied rotation speed range.

Keywords*:* Polymers, Thermoplastics, Polyetherimide, Friction Riveting, FricRiveting, Thermal degradation, Microtomography.

1. Introduction

Amorphous polyetherimide (PEI) is a high-performance thermoplastic polymer developed in the 1970s by Wirth et al [2] and first commercialised in 1982 [3]. Their chemical structure consists of repeating aromatic imide, propylidene (isopropylidene) and ether groups, as seen in Figure 1. While the aromatic imide groups are responsible for polymer stiffness and high thermal resistance, the ether groups provide PEI good processability associated with low melting viscosities [4].

PEI is primarily used in the automotive, electrical/electronic, medical, packaging, aircraft and industrial markets [4-8] in the form of sheet and moulded parts. In aerospace applications, particular advantages are their inherently flame retardant behaviour, low smoke emission and chemical resistance against most fuels and fluids [9]. One remarkable thermal property of PEI resins is their high softening point, represented by the glass transition temperature in the order of 215 to 220 ^{o}C [3]. PEI resins can be processed with most conventional thermoplastic techniques. High melting processing temperatures are needed, ranging from 350°C to 425°C [10] and granulates are normally dried prior to melt processing, because of its relative high water absorption [3,11].

The high processing temperatures plus the low coefficient of thermal expansion makes PEI a good candidate for joining technology applications [12-14]. However, thermal processing, such as that found during welding and

thermal bonding, is well known to cause a certain extension of thermal degradation, due to the high temperatures and dwell times. The thermal degradation in PEI was extensively studied in the last decades [15-22]. PEI can basically undergo thermal degradation in two ways: by random scission or by crosslinking [23]. Decreasing molecular weight (MW) may result in inferior polymer strength. Conversely, crosslinking will augment polymer strength. While the increase of MW improves yield strength, it also increases molten viscosity [19]. Crosslinking in PEI was reported to occur in temperatures ranging from 320-380^{o}C [15,19], whereas chain scission above 400 ^{o}C shows a maximum rate of decomposition (rate of weight loss) around 510-540 ^{o}C [15-20]. Chain scission happens in two stages for PEI: an early stage at 520 ^{o}C, where the isopropyledene moieties, ether linkages and phenyl-phthalimides rings are broken, and a less pronounced stage above 600 ^{o}C, producing CO_2 and water by heat-induced hydrolysis of phthalimide rings [17]. The FricRiveting process temperatures are usually found to lay within the early stage of degradation of the studied PEI [24].

The accepted thermal degradation reactions taking place for the studied PEI are presented in Figures 2 and 3. Reactions T_1 and T_2 (Figure 2) represent the scission followed by C-H hydrogen-transfer reactions at the ether linkages. This results in compounds containing phthalimide units with the phenyl rings substituted by H/OH and/or bisphenol-A. Reaction T_3 consists of the disproportion of the isopropylidene moieties in the bisphenol-A units, followed by hydrogen transfer reactions. This results in the formation of compounds containing intact phthlimide rings with ether linkages, hydrogen, methyl, ethyl,

isopropylidene and isopropyl end-groups (R) (R equals to H, CH_3, C_2H_5, C_3H_5, C_3H_7). If the working atmosphere is rich in oxygen, T_3 reaction may follow complex thermo-oxidative reactions leading to the formation of compounds such as alcohols, acetones and acids [22,25]. Finally, reaction T_4 corresponds to scission of phenyl-phthalimide bonds followed by hydrogen transfer resulting in compounds with N-H and or N-phenyl end-groups.

The crosslinking mechanisms of PEI ULTEM 1000 are currently not well understood. Kuroda et al. [15] have proposed that links between chains are probably formed by combination of two radicals resultant from the chain scission (β-scission) of isopropylidene moieties followed by the substitution of phenyl radical into benzene. A schematic representation of a crosslinked region originated by such mechanisms is found in Figure 3.

Recently, thermoplastic PEI was demonstrated to be joinable by FricRiveting [26]. This new joining technology developed in 2005 [1] was conceived for assembling thermoplastics and thermoplastic matrix composites with lightweight alloy parts. In this process two or more pieces are kept together by a round rivet, which is mechanically anchored by means of frictional heating resultant from high rotation speeds and axial pressures applied on the rivet. As a matter of illustration the process can be represented by the point-on-plate joint in Figure 4, where a metallic rivet is inserted into a thermoplastic base plate. Prior to joining, the pieces are firmly fixed in the joining machine (Figure 4A). The rotating rivet is than pressed against the base plate. Friction will increase temperature in the rubbing area so a thin layer of

softened/molten polymer will be created. This allows the rotating rivet starting penetrating the base plate, pushing off softened/molten polymer as flash (Figure 4B). Due to the low thermal conductivity conditions the temperature highly increases in the rubbing area and the tip of the rivet becomes plasticized. At this point a higher axial pressure is applied on the rivet. The plasticized tip of the rivet will deform as a result of its interaction with the colder volumes on the base plate (Figure 4C). After cooling under pressure, joint consolidates and a strong joint is obtained by mechanical anchoring and adhesion holding forces [24].

Although the FricRiveting process is characterized by short heating times (typically from 0,5 to 10 s), high process temperatures are achieved, which are generally in the degradation range of the polymeric partner. Considering that the thermal degradation is directly coupled with mechanical performance in plastics, this should be avoided or minimized in order to guarantee joint mechanical integrity in FricRiveting. In the part-I of this two-fold work, the influence of process temperature on the thermal degradation behaviour of an extruded amorphous PEI was experimentally determined for variable rotation speeds during FricRiveting. For this purpose gel permeation chromatography (GPC), Fourier transform infrared spectroscopy (FTIR) and synchrotron based X-ray microtomography, where selected to determine the amount of degraded/thermally changed material in the polymeric portion of the friction riveted joints. The second part article will additionally present the influence of joining time and pressure on thermal degradation mechanisms of the friction riveted PEI.

2. Experimental

2.1. Materials

Commercial available 13,4 mm extruded amorphous thermoplastic polyetherimide (PEI ULTEM 1000, GE Plastics) plates were friction riveted by Φ5 mm aluminium 2024-T351 ($AlCu_4Mg$) round rivets in the point-on-plate configuration.

2.2. Sample preparation

With the aim of creating variable processing temperature conditions, joints were produced by keeping setup joining time and joining pressure constant at 3 s and 1,1 MPa (11 bar) respectively, while rotation speed was varied within 1570 – 2199 rad/s (15000 - 21000 rpm). The joining equipment and procedures are described elsewhere [24]. Joints in this working range exhibited good tensile and shear strength [27]. Tiny slices of thermally processed polymer material from 4 different joints (rotation speed conditions 1570,8 rad/s, 1780,2 rad/s, 1989,7 rad/s and 2199,0 rad/s) were extracted with a scalpel at room temperature from the expelled softened/molten flashes, after joint consolidation (Figure 5), for analytical investigation.

2.3. Gel permeation chromatography (GPC)

GPC-experiments were carried out in a equipment constituted by a HPLC-pump 515, autosampler 717 plus a vertical heating furnace, a dual λ absorbance detector 2487 and dual refractive index detector 2414 (Waters); a polystyrene-divinylbenzene 5 μm column (mod. Styragel HR 5, 4, 3, Waters) and a PC-based evaluation software (Empower, Waters) completed the system. Samples of approximately 8 mg were diluted in 4 mL of dimethylformamide, DMF (Nr. D/3846/PB17, Fisher) with 0,05 M LiBr (Nr. 13008, Riedel-de-Haën) under stirring at room temperature during 24h, and finally filtered (0,45 μm polyamide filter). GPC-system calibration was performed with polymethylmetacrylate, PMMA, standards (Polymer Lab).

2.4. Synchrotron X-ray computer tomography (μCT)

Microtomographic testing was performed at GKSS Forschungszentrum's high-energy synchrotron beamline (HARWI-2) at Hamburger Synchrotronstrahlungslabor (HASYLAB) of the Deutsches Elektronen-Synchrotron (DESY), Hamburg, Germany. A complete description of this μCT set-up is found elsewhere [28]. In this investigation Φ15 mm cylindrical μCT-samples were machined down from the centre of the joint, as

represented in Figure 6. FricRiveting samples were scanned by using 36 keV photon energy. Samples volume rendering and quantitative measurements were performed with the image analysis VGstudiomax software (Volume Graphics, Heidelberg, Germany).

2.5. Fourier transform infrared spectroscopy (FTIR) and differential scanning calorimetry (DSC)

FTIR (ATR) infrared spectra of PEI slices (2 mg) were recorded on a Bruker Equinox IFS 55 spectrophotometer in the range 4000-400 cm^{-1}. The spectra were fitted to evaluate the peaks area within the wave number range of 3000-600 cm^{-1}. DSC-thermograms for the glass transition determination of the untreated PEI samples (13 g) were obtained from a Netzsch DSC 204 equipment. A temperature range of 20-350 ^{o}C plus a heating rate of 20 K/min were chosen; samples were placed in Al-pans and scanned in N_2 inert atmosphere (55 mL/min) within a 500 μV range. T_g values were calculated based on ISO 11357-1 [29].

2.6. Process temperature evaluation

An infrared thermography system constituted of an infrared thermo-camera (VarioTHERM, Jenoptik GmbH [30]) connected to a computer with own data acquisition and treatment software, was used for evaluating process temperature. Aluminium rivets were painted with black paint and PEI plates were covered with a black painted cardboard-shield in order to minimise measurements interference related to aluminium low emissivity, and PEI semi-transparency. Temperature data was collected during joining from the pushed off molten polymer flash with a working distance of 260 mm (distance from the measured area to the centre of objective) and an incidence angle of 15^{o} (Figure 7).

3. Characterization of the untreated polyetherimide

The calculated average numeric weight (Mn) of (2,6 ± 2) 10^5 g/mol and weight molecular weight (Mw) of (5,22 ± 0,01) 10^5 g/mol measured by GPC for 2 samples of the used PEI are in the range reported before for the commercial polymer [4].

The untreated PEI (2 samples) was also evaluated by FTIR. The assignment of the main peaks in experimental FTIR spectrum (Figure 8) is shown in Table 1. The PEI characteristic absorption peaks for the imide (e.g.

carbonyl and amine stretching in the phthalimide rings), ether (e.g. aryl-ether-aryl stretching) and propylidene groups (e.g. carbon-hydrogen stretching in the aromatic rings) were successfully identified (Table 1). Finally, the DSC-investigation also indicated that the glass temperature range is in accordance to the literature [3], with an average value of 221,0 ^{o}C (Figure 9).

4. Results and discussions

4.1. Influence of increasing rotation speed on the process temperature

In order to evaluate the temperature profile during the joining process, 2 joints per condition were analysed by infrared thermography. The temperature measurements carried out in the polymer flash is a good indicator of how high is the temperature of the softened polymer layer in the rubbing area. Due to the low thermal conductivity of the polymer, it is assumed that the polymer softened through frictional heating and pressed off as flash will not have enough time to cool down before it leaves the polymer base plate. In other words, the average temperature measured in the softened flash is considered nearly the same as in the molten layer inside the polymer plate.

Average process temperature evaluated by infrared thermography are presented in Figure 10. Figure 10A shows a sharp increase in the flash temperature within the first 3 seconds (the setup joining time for these

samples) indicating high heating rates. Slower cooling rates for these joints are associated with the natural cooling under room temperature. Figure 10B presents the peak temperatures extracted from the temperature vs. time curves in Figure 10A. A clear trend of increasingly temperature with the rotation speed could be observed as a result of the friction energy being transformed in heat and the low thermal conductivity of the polymer. Peak temperatures for the tested rotation speeds were well above the average glass transition temperature of the PEI polymer (221,0 ^{o}C) approximately varying in the range of 350-475 ^{o}C, which is within the initial range of thermal degradation by chain scission for the studied polymer [15-20]. In addition to that, the average relative increase of about 2 ^{o}C per 100 rad/s (20 ^{o}C per 1000 rpm) shows the importance of the rotation speed to achieve the FricRiveting temperature.

4.2. Thermal degradation behaviour of friction riveted PEI polymer

It is well known that thermal degradation during thermal processing is highly influenced not only by the applied temperature but also by the dwell time and heating rates. Aiming to determine the thermal degradation behaviour of the friction riveted PEI polymer under increasingly rotation speed, the analytical techniques GPC, FTIR and X-ray computer microtomography were selected and their results analysed as a function of peak temperature, heating rate and heating time (the monitored time is considered the time between the initial

contact of the rotating rivet with the polymeric base plate and its complete stopping).

For establishing the nature of thermal degradation mechanisms taking place during joining, specimen molecular weight distributions (Figure 11A) and polydispersivity (Figure 11B) were analysed. Only a slightly broader curve was measured after processing, with a slightly higher content of low MW polymer, when elevating rotation speed (Figure 11A). Taking into account this observation and the process temperature, it is possible to conclude that the main thermal degradation mechanism taking place during joining is chain scission instead of cross linking. A crosslinked structure would preferentially lead to an increase of MW [19]. This behaviour can be also confirmed by the increase of polydispersivity with rotation speed (Figure 11B), probably owing to the presence of smaller scissioned entities.

Figure 12A shows the number average (Mn) and weight average (Mw) molecular weights values as a function of rotation speed plotted from their normalization with the untreated polymer molecular weight (M/M_{PEI}) in comparison to experimental peak temperature, heating rate and heating time (Figure 12B). One can observe from Figure 12A that the declining in average molecular weight was low (about 3% for Mn and Mw) in the temperature range of about 350-450 ^{o}C (1570,8 – 1989,7 rad/s) and moderate (about 10,0% for M_n and 5,0 % for M_w) at 500 ^{o}C (2199 rad/s). This behaviour can be understood when analysing Figure 12B. Although high average peak temperatures and heating rates (92-160 ^{o}C/s) were detected, the heating time

(corresponding to dwell time for thermal degradation) seems not to be high enough to induce a large amount of chain scissioning in combination with the former parameters, for the tested rotation speed range.

Sanner et al. [45] studied the effect of different molecular weights in the PEI ULTEM's mechanical properties. For a molecular range varying from M_n = 15660 to 22820 g/mol and M_w = 36640 to 52300 g/mol, the tensile strengths at temperatures ranging from 23 - 140 ^oC were not strongly altered. Considering that untreated PEI used in this work had average molecular weights similar to those studied by those authors (Mn = 26332 g/mol and Mw = 52234 g/mol), the decrease of about 10% for Mn and 5% for Mw (Mn=22250 g/mol and Mw=49650 g/mol) in average molecular weight measured by GPC can be considered as irrelevant to the global tensile strength. The experimental values of MW for the studied samples lay either above or within the molecular weight range of PEI where tensile strength behaves independently of this property (Figure 13).

Yet this conclusion should be taken with caution considering that the nature of the chain scission process for the thermo-mechanically degraded samples is not well defined. A closer analysis of MW distribution curves in Figure 11A may suggest that a random chain scission process occurred (curves shifting to the low MW side or longer elution times). In normal conditions, this would imply that even small variations in average MW would be responsible for changes in polymer strength, which was not the case for the samples in this work. The irrelevance of the decreasing molecular weight in the

behaviour of global mechanical strength for the studied joints was demonstrated elsewhere [24]. A broader conclusion in the complex thermo-mechanical behaviour of the joined PEI would require a more elaborated analytical investigation of the MW distribution curves, which is out of the scope of this work.

The evaluation of degradation was further investigated by FTIR spectroscopy. The FTIR-spectra of the investigated specimens are presented in Figure 14. From a first observation of this figure it is difficult to identify changes in intensity of the FTIR peaks of riveted specimens.

A better way of evaluating changes in the intensity of FTIR peaks can be achieved by deconvulating the spectra and calculating the evolution of the main affected polymer absorptions versus a thermally stable peak, by means of determining the normalized peak areas in comparison to the untreated polymer (A_{peak}/A_{base}). Particularly for this PEI polymer Musto et al [46] identified that the peaks related to the propylidene groups as well as those ones associated with carbonyl groups and phthalimide groups are normally altered by thermal treatment, where higher temperatures lead to drops in their intensities. Figure 15 shows the behaviour of the FTIR peaks areas 3070 cm^{-1} and 2968 cm^{-1} (CH-stretching propylidene moieties), 1779 cm^{-1} (carbonyl stretching phthalimide groups),1715 cm^{-1} and 1612 cm^{-1} (amine stretching phthalimide groups), and 1070 cm^{-1} (stretching aryl-ether-aryl bonds) normalized by the area of thermally stable peak 838 cm^{-1}(vibrations of aromatic groups) versus rotation speed. From this plots, one can observe that, though

weak, there is a trend in decreasing the normalized absorption areas when increasing rotation speed, temperature, heating rate and heating time (see Figure 12B). This helps to confirm the GPC results where heating time were not enough to cause high levels of chain scissioning (decrease in spectra analysed peak areas) although high peak temperatures and heating rates were present.

Finally the X-ray computer microtomography was used attempting to evaluate and quantify thermal degraded PEI material for the comparative rotation speed specimens. The cylindrical samples had their full volume rendered and divided into 3 main volume parcels, as represented in Figure 16. The total volume of the joint (the first volume entity in Figure 16A) contains the PEI polymer (volume in green, Figure 16) and the volumetric defects (the second volume entity in yellow, Figure 16B) around the deformed rivet. The volume of the deformed metallic rivet (in red, Figure 16C) is the third volume entity.

As the central focus of this tomographic investigation, the volumetric defects were isolated and quantified for each specimen. Volumetric defects are considered to be flaws associated with thermo-mechanical treatment from the processing. These can be either thermal degraded material, volatile formation pores or some entrapped air bubbles due to the high shear rates involved in the process.

These flaws can drastically reduce short- and long term mechanical performance of the joint and should be avoided. Unfortunately, in the case of a

process where high temperature regimes are present, such as hot-tool welding, resistance welding, induction welding and FricRiveting, volumetric defects will be inherently present [47], so one can only reduce their density but not fully eliminate them. It has been reported that PEI has a significant affinity for atmosphere moisture [48]. While for the majority of the polymers it would negatively affect short-term mechanical properties, moisture does not considerably affect PEI strength [49]. Nevertheless, under high temperatures ($T > T_g$), high heating rates, and increasing heating time, desorption of moisture and other volatiles in the polymer structure can lead to nucleation and growth of voids [47], in addition to flaws associated with chain scissioning and entrapped air. The separation of these types of flaws is a very complex matter and is out of the scope of this work. Furthermore, it has been demonstrated [24] that these effects have the lowest influences on volumetric defects formation so in the current analysis, volumetric defects are considered only as thermal degraded material.

The determination of volumetric defects (V_d) has been performed through the calculation of ratios among V_d and the total volume of the specimen (V_T). This sort of volume normalization allows the direct comparison between different segmented volumes. Figure 17 illustrates the V_d-quantitative results. Increasingly rotation speeds created only a very small fraction of flaws (in average less than 1% of the total volume of the specimen) and did not induce substantial measurable alterations (Figure 17). It might suggest that increasingly rotation speed does not strongly influence thermal degradation, at least in the studied parameter range for this combination of materials. This is

once more in agreement with the results for the GPC and FTIR investigations, where thermal degradation was restricted to low amounts, mainly due to the low experienced dwell times, even when high temperatures and heating rates were observed.

4. Conclusions

It has been demonstrated that the rotation speed plays a important role on controlling the temperature evolution, heating rate and heating time during FricRiveting of PEI and Al 2024 alloy. The temperatures measured in the fresh expelled polymeric material had peak values around 350-475 ^{o}C, which are above the range of chain scissioning thermal degradation regime for the PEI polymer. Consequently, thermally degraded material will be present inside the joint, which can be prejudicial to the integrity of joint mechanical properties. Temperature and heating rates were found to increase with the rotation speed, while the heating time (in this case assumed to be the thermal degradation dwell time) increased only slightly. Thermal degradation on the other hand was observed to be less influenced by increasingly rotation speeds. GPC molecular weight measurements showed that the main thermal degradation mechanism is the chain scissioning, with very small decrease in average molecular weight (10% for Mn and 5 % for Mw at 2199 rad/s) within the studied rotation speed range. Although variations in average MW normally influence polymer strength, this was not observed for the investigated joints [24]. This minor decrease in molecular weight can be considered irrelevant for the mechanical performance

of the joints because it is either above or within the molecular weight range where the strength of the PEI polymer is independent of the variations in this property [45]. The thermal degradation behaviour was further studied by FTIR analysis. The minor drops in the absorbance areas of the peaks related with the main groups of PEI polymer (3070, 2968, 1779, 1715 and 1612 cm^{-1}), when elevating the rotation speed, additionally indicated that, thermal degradation by chain scissioning was very small. The μCT investigation helped to support the conclusions on polymer thermal changes as a function of rotation speed. Additionally, the μCT analysis served to identify that the thermal related volumetric flaws were located around the deformed rivet. This analysis also helped to confirm that the rotation speed has only a limited influence on thermal deteriorated material formation (generally less than 1 % of volumetric defects in the joint) in the studied parameter range for this combination of materials. This behaviour can be associated with the shorter measured heating times (< 3 s) although the good stability of the thermoplastic PEI certainly contributes to the low level of thermal degradation. Therefore, it was demonstrated that rotation speed has a weak influence on the thermal degradation of the studied joints. The results obtained in this work (i.e. the influence of variable rotation speed on process temperature and thermal degradation mechanisms) may be extended to other engineering thermoplastics being friction riveted by aluminium rivets. Finally, the understanding of the thermal degradation mechanisms in the FricRiveting helps to predict and model the mechanical performance of the joints, leading to time and cost savings.

5. Acknowledgements

The authors would like to acknowledge the financial support provided to S.T. Amancio-Filho by the Conselho Nacional de Pesquisa CNPq – Brazil (GDE Proc.Nr. 20000/06-03).

6. References

1. Amancio Filho ST, Beyer M, Dos Santos JF. Verfahren zum Verbinden eines metallischen Bolzens mit einem Kunststoff-Werkstück – DE 10 2005 056 606 A1. Germany: Deutsches Patent- und Markenamt, 2007.

2. Wirth JG, Heath DR. US Patent 3.730.946. USA: American Patent Office, 1973.

3. ASM Engineering Plastics 1st ed. Engineered Materials Handbook Vol. 2. ASM International, 1988.

4. Serfaty W. Polyetherimide: a versatile, processable thermoplastic. In Polyimides, synthesis, characterization, and applications. Mittal KL., editor. New York: Plenum Press, 1984. p. 149.

5. Keeping technology moving, Lexan and Ultem film and sheet: Advanced engineering materials for the transportation industry. GE Plastics Specialty Film & Sheet at http:// www.geplastics.com, January 2006.

6. GE Plastics launches new aircraft interior materials at Aircraft Interiors Expo – May 2006. at http://www.composites world.com/news/cwweekly/2006/May.htm, May 2006.

7. Westland 30-300 thermoplastic tailplane. Plastics and Rubber International 1987;12(1):23-24.

8. Ginger G. Thermoplastic composites gain leading edge on the A380. High Performance Composites 2006;March:50-55.

9. ASM Handbook. Engineering Plastics 1st. ed. Engineered materials handbook vol.2. USA:ASM International, 1988.

10. Brydson JA. Plastic materials 7th ed.. USA:Butterworth Heinemann, 1999.

11. Long Jr ER, Collins WD. The effects of fluids in the aircraft environment on a polyetherimide. Polym Eng Sci 1988;28(12):823-828.

12. Ageorge C, Lin Y, Meng H. Experimental investigation of the resistance welding for thermoplastic-matrix composites. Part II: optimum processing window and mechanical performance. Comp Sci Tech 2000;60:1191-1202.

13. Stokes V K. Experiments on the jot-tool welding of three dissimilar thermoplastics. Polymer 1998;39(12):2469-2477.

14. Stokes V K. Vibration weld strength data for glass-filled polyetherimide. J Adhes Sci Tech 2001;15(14):1763-1768.

15. Kuroda SI, Terauchi K, Nogami K, Mita I. Degradation of aromatic polymers – I. rates of crosslinking and chain scission during thermal degradation of several soluble aromatic polymers. Eur Poly J 1989;25(1):1-7.

16. Torrecillas R, Baudry A, Dufay J, Mortaigne B. Thermal degradation of high performance polymers – influence of structure on polyimide thermostability. Poly Degrad Stabil 1996;54:267-274.

17. Caroccio S, Puglisi C, Montaudo G. Thermal degradation mechanisms of polyetherimide investigated by direct pirolysis mass spectroscopy. Macrom Chem Phys 1999;200:2345-2355.

18. Perng L.H. Thermal Degradation Mechanisms of Poly(ether imide) by stepwise Py-GC/MS. J Appl Poly Sci 2001;79:1151-1161.

19. Augh L, Gillespie Jr JW, Fink BK. Degradation of continuous carbon-fiber reinforced polyetherimide composites during induction heating. J Thermoplast Compos Mater 2001;14:96-115.

20. Barbosa-Coutinho E., Salim VMM, Borges CP. Preparation of carbon hollow fiber membranes by pyrolysis of polyetherimide. Carbon 2003;41:1707-1714.

21. Harinaht VA, Lou J. Characterization of the thermo-oxidative stability of filled thermoplastic polyetherimide. Presentation in IMECE`03 ASME

International Mechanical Engineering Congress, 15-21 November, Washington, 2003.

22. Caroccio S, Puglisi C., Montaudo G, New vistas in polymer degradation. Thermal oxidation processes in poly(ether imide). Macromolecules 2005;38:6849-6862.

23. Schnabel W, Polymer Degradation, principles and practical applications., Berlin:Akademie-Verlag, 1981.

24. Amancio Filho ST. Friction Riveting: development and analysis of a new joining technique for polymer-metal multi-materials structures, PhD Thesis. Hamburg: Technical University of Hamburg-Harburg, Department of Mechanical Engineering, Institute for Materials Science and Technology, 2007.

25. Caroccio S, Puglisi C, Montaudo G, Comparison of Photooxidation and thermal oxidation processes in poly(ether imide). Macromolecules 2005;38:6863-6870.

26. Amancio Filho ST, Dos Santos JF. Beitrag zur Entwicklung eines neuen Fügeverfahrens für Kunststoff und Leichtbaulegierungen. Proceedings Geesthachter Schweißtage `06 – Festphase-Fügeverfahren Conference 2006;1:145-150.

27. Amancio-Filho ST, dos Santos JF. Friction Riveting: a new tool for joining and fabricating polymer-metal multi-materials structures. Submitted to Comp Sci Tech, 2007.

28. Bernhardt R, Scharnweber D, Müller B, Beckmann F, Goebbels J, Jansen J, Schliephake H, Worch H. New developments for synchrotron-radiation-based microtomography at DESY. Proceedings SPIE conference, paper 6318, USA, 2006.p. 7-17.

29. ISO 11357-1, Plastics – Differential scanning calorimetry (DSC) – Part 1: General principles. 1997.

30. VarioTherm - Einführung in Theorie und Praxis der Infrarot-Thermografie. Infra Tec GmbH, Dresden, Germany, 2005.

31. Kuroda SI, Mita I. Degradation of aromatic polymers – II. The crosslinking during thermal and thermo-oxidative degradation of a polyimide. Eur Poly J 1989;25(6):611-620.

32. Lambert JB. Introduction to organic spectroscopy New York:Prentice Hall, 1987.

33. Sundar S, Aruna P, Venkateshwarlu U, Radhakrishnan G. Aqueous dispersions of polyurethane cationomers: a new approach for hydrophobic modification and crosslinking. Colloid Poly Sci 2004;283:209-218.

34 Bijwe J, Tewari US, Vasudevan P. Friction wear studies of bulk polyetherimide. J Mater Sci 1990;25:548-556.

35. Gardner SH. An investigation of the structure-property relationships for high performance thermoplastics matrix, carbon fiber composites with a

tailored polyimide interphase. Blacksburg: Virginia Polytechnic Institute and State University, 1998.

36. Guerra G, Chloe S, Williams DJ, Karasz FE, MacKnight WJ. Fourier Transform Infrared Spectroscopy of some miscible polybenzidazole/polyimide blends. Macromolecules 1998;21:231-234.

37. Hummel DO, Göttgens S, Neuhoff U, Düssel HJ. Linear-temperature programmed pyrolysis of thermoresistant polymers – mass and FT-IR spectrometries; Part 3. poly(1,4-phenylene terephthalamide) and aromatic polyimides. J Anal Appl Pyrol 1995;33:195-212.

38. Seo Y, Hong SM, Hwang SS, Park TS, Kim KU, Lee S, Lee J, Compatibilizing effect of a poly(esterimide) on the properties of the blends of poly(ether imide) and a thermotropic liquid crystalline polymer: 1. Compatibilizer synthesis and thermal and rheological properties of the in situ composite system. Polymer 1995;36(3):515-523.

39. Pramoda KP, Chung TS, Liu SL, Oikawa H, Yamaguchi A. Characterization and thermal degradation of polyimide and polyamide liquid crystalline polymers. Polymer Degradation and Stability 2000;67:365-374.

40. Vora RH, Pallathadka PK, Goh SH, Chung TS, Lim YX, Bang TK. Preparation and characterization of 4,4´-bis(4-aminophenoxy)diphenyl Sulfone based fluoropoly(ether-imide)/organo-modified clay nanocomposites. Macromol Mater Eng 2003;288:337-356.

41. Kurdi J, Kumar A. Structuring and characterization of a novel highly microporous PEI/BMI semi-interpenetrating polymer network. Polymer 2005;46:6910-6922.

42. Choukourov A., Hanuš J, Kousal J, Grinevich A, Pihosh Y, Slavínská D,. Biederman H. Thin polymer films from polyimide vacuum thermal degradation with and without a glow discharge. Vacuum 2006;80(8):923-929.

43. Sundar, S., Jang W, Lee C, Shul Y, Han H. Crosslinked sulfonated polyimide networks as polymer electrolyte membranes in fuel cells. J Poly Sci: B 2005;43:2370-2379.

44. Pryde CA. IR studies of polyimides. I. Effects of chemical and physical changes during cure. J Poly Sci A 1989;27:711-724.

45. Sanner MA, Haralur G, May A. Effect of molecular weight on brittle-to-ductile transition temperature of polyetherimide. J Appl Poly Sci 2004;92:1666-1671.

46. Musto P, Karasz FE, MacKnight WJ. Fourier transform infrared spectroscopy on the thermo-oxidative degradation of polybenzimidazole and of a polybenzimidazole/polyetherimide blend. Polymer 1993;34(12):2934-2945.

47. Roychowdhury S, Gillespie Jr JW, Advani SG. Volatile-induced void formation in amorphous thermoplastic polymeric materials: I. Modelling and parametric studies. J Compos Mater 2001;35(4):340-366.

48. Merdas I, Thominetti F, Verdu J, Humid Aging of Polyetherimide. II. Consequences of water absorption on thermomechanical properties. J Appl Poly Sci 2000;77:1445-1451.

49. Sepe MP. The effect of absorbed moisture on the elevated temperature properties of polyetherimide. Proceedings Society of Plastic Engineers' Antec 2004, 2236-2240.

Figures

Figure 9. Experimental DSC-thermogram showing the glass transition temperature range calculated for the polymer PEI Ultem 1000.

Figure 10. (A) infrared temperature measured during FricRiveting for the investigated joints. (B) plot with the peak temperatures extracted from (A), versus rotation speed.

Figure 11. (A) Size exclusion chromatography (SEC) molecular weight distributions for investigated rotation speed specimens. (B) Influence of rotation speed on SEC polydispersivity of studied specimens.

Figure 12. GPC average numeric (Mn) and molecular weights (Mw) normalized by the average PEI Ultem 1000 untreated polymer. (B) infrared peak temperatures, heating rates and heating times plotted versus rotation speed.

Figure 13. Experimental molecular weight results plotted over the molecular weight intervals (hatched areas) where the tensile strength of PEI Ultem 1000 is not strongly influenced by this variable [45].

Figure 14. FTIR spectra of the investigated FricRiveting polymer specimens: A) wavenumber range from 3250 to 2850 cm^{-1}. B) wavenumber range from 1875 to 550 cm^{-1}.

Figure 15. FTIR absorbance peaks normalized with the stable 838 cm^{-1} peak (aromatic ring vibrations) plotted versus rotation speed.

Figure 16. Example of a μCT volume-renderized friction riveted PEI/Al2024 joint. (A) the total volume including the volumetric defects shown in (B) and the deformed tip of the metallic rivet represented in (C).

Figure 17. Normalized μCT volumetric defects (V_d/V_T) caused by thermal treatment during FricRiveting plotted versus variable rotation speed. The rendered figures of the analysed V_d are depicted over the curve.

Table

Table 1. Major infrared absorbance peaks of the base material polyetherimide PEI Ultem 1000 in Figure 8.

Table 1

Click here to download high resolution image

Wavenumber [cm^{-1}]	Peak Intensity	Assignment
3060	weak	C-H, stretching (aromatic rings) [31,32]
2970, 2930, 2875	weak	C-H stretching (propylidene moieties) [31,33,46]
1777, 1715	medium to strong	C=O, carbonyl stretching (in phthalimide rings) [31 33-41]
1598	medium	C=C or C-N stretching [32,42]
1476	medium	Aromatic ring stretching [39,42]
1348	strong	C-N stretching (in phthalimide rings) [32-34,37-40, 42,43,46]
1262, 1232, 1070, 1013	strong to medium	Ar-O-Ar stretching (aryl (Ar) ether bonds) [32,37 39-42]
833	medium	Aromatic ring deformation vibrations [42,44]
740	medium	Phthalimide ring bending vibrations [31,38,40,43,44]

Figure 1

Click here to download high resolution image

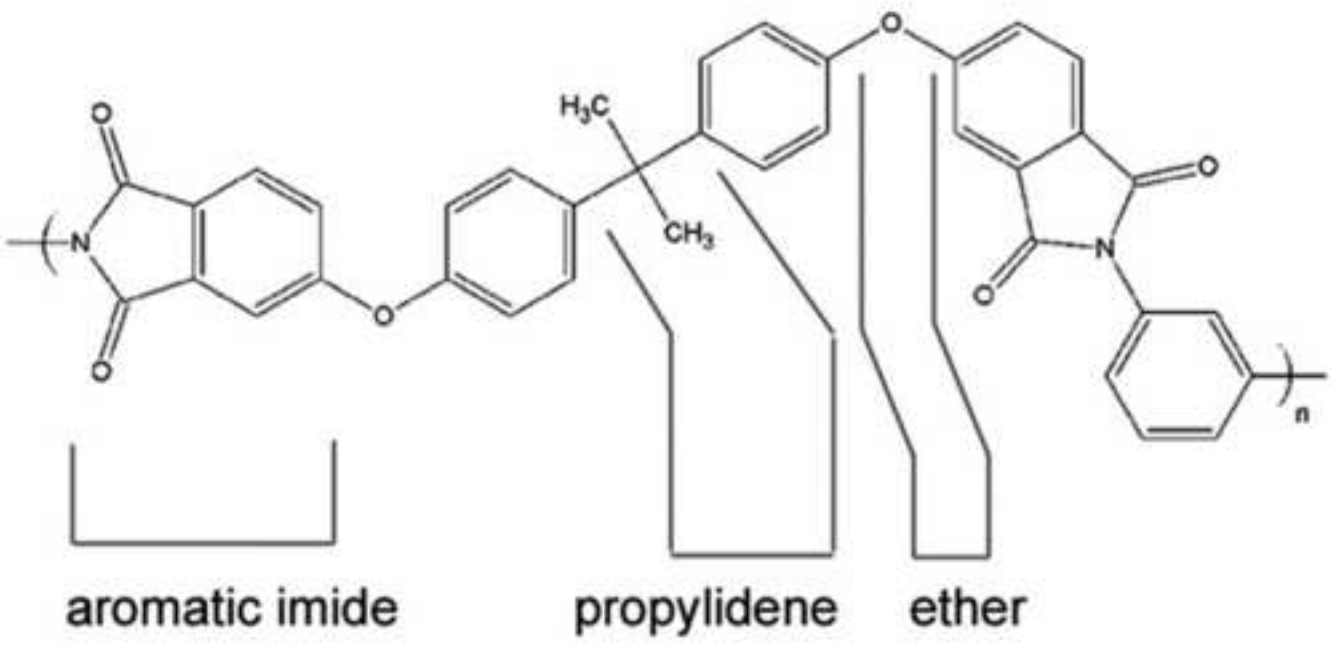

Figure 2

Click here to download high resolution image

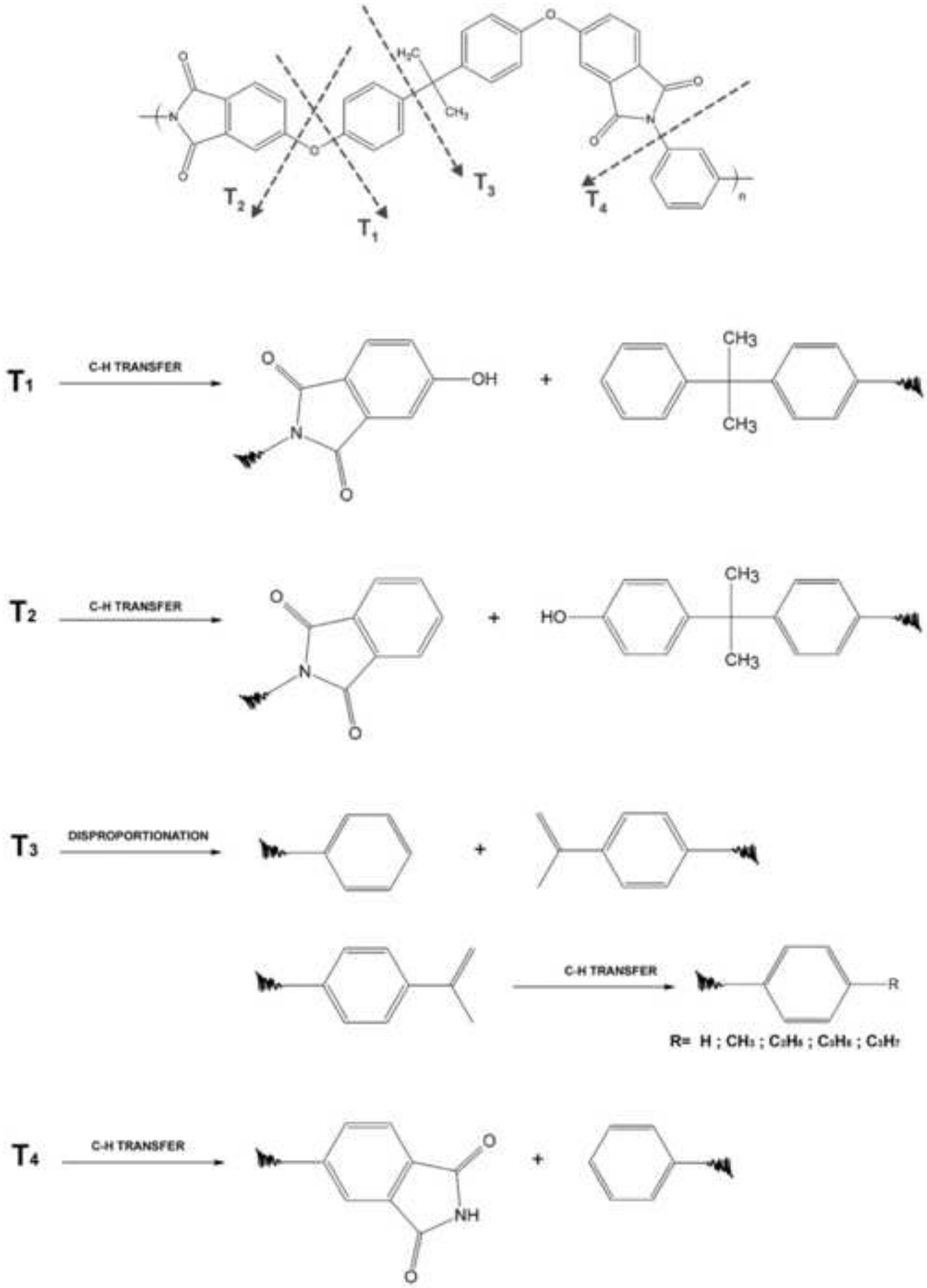

Figure 3

Click here to download high resolution image

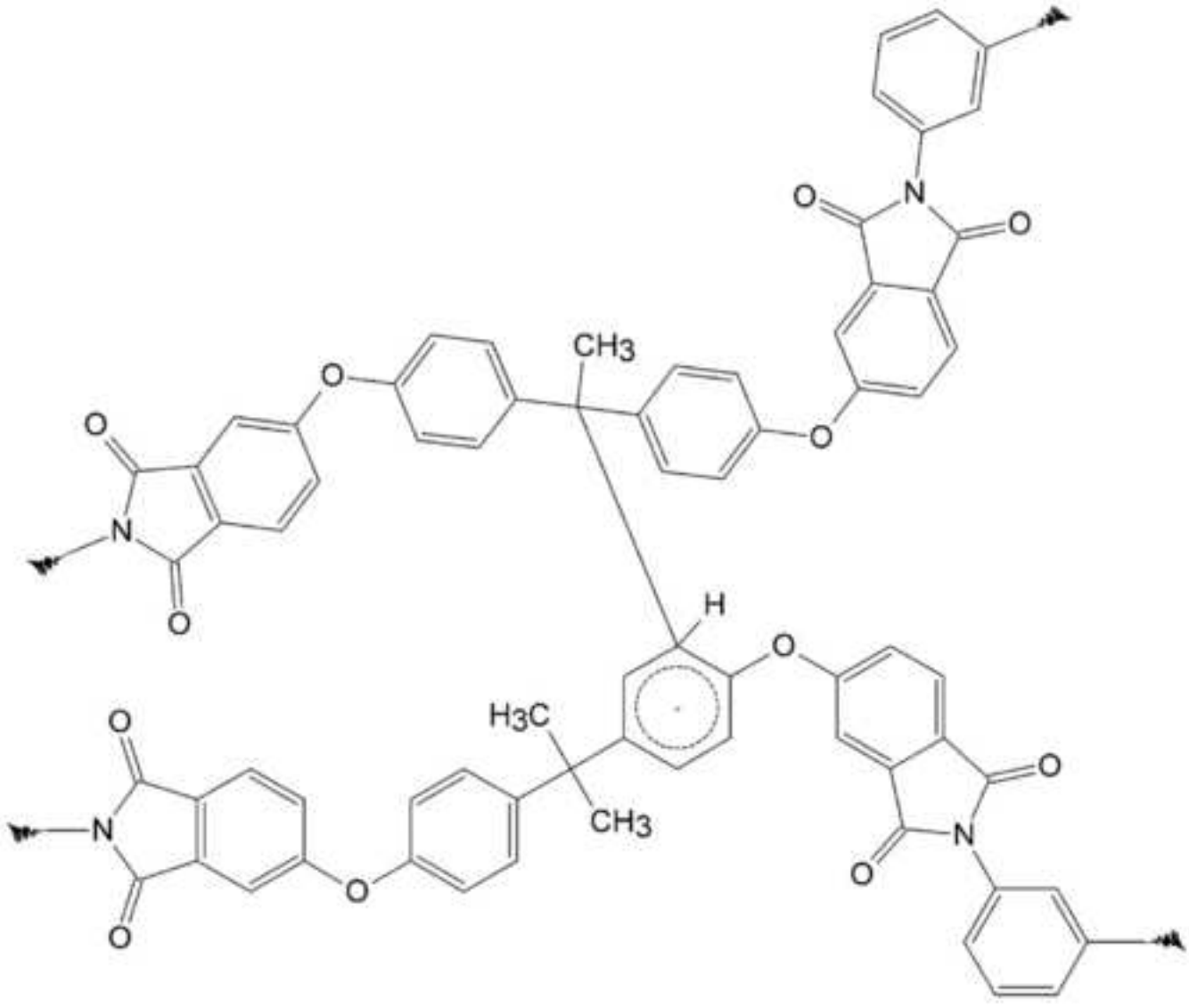

Figure 4

Click here to download high resolution image

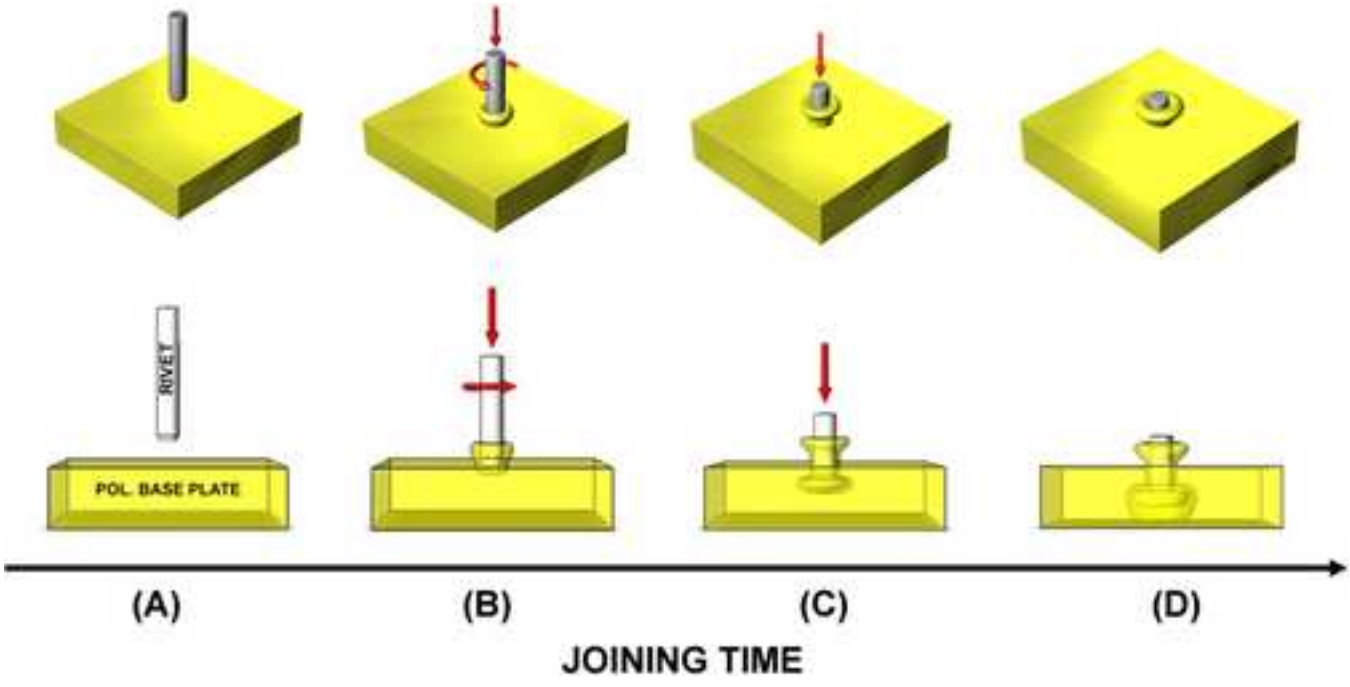

Figure 5

Click here to download high resolution image

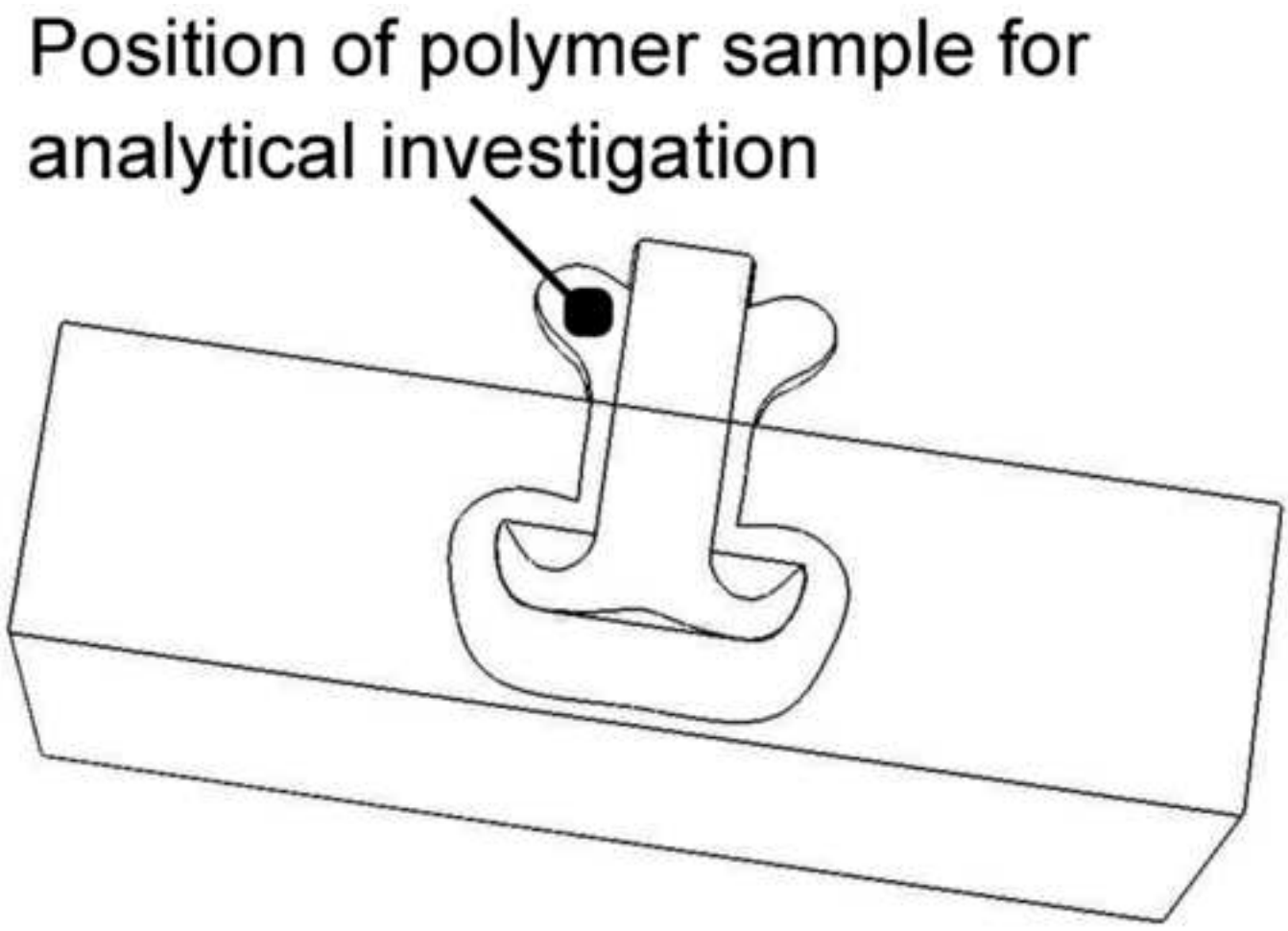

Figure 6

Click here to download high resolution image

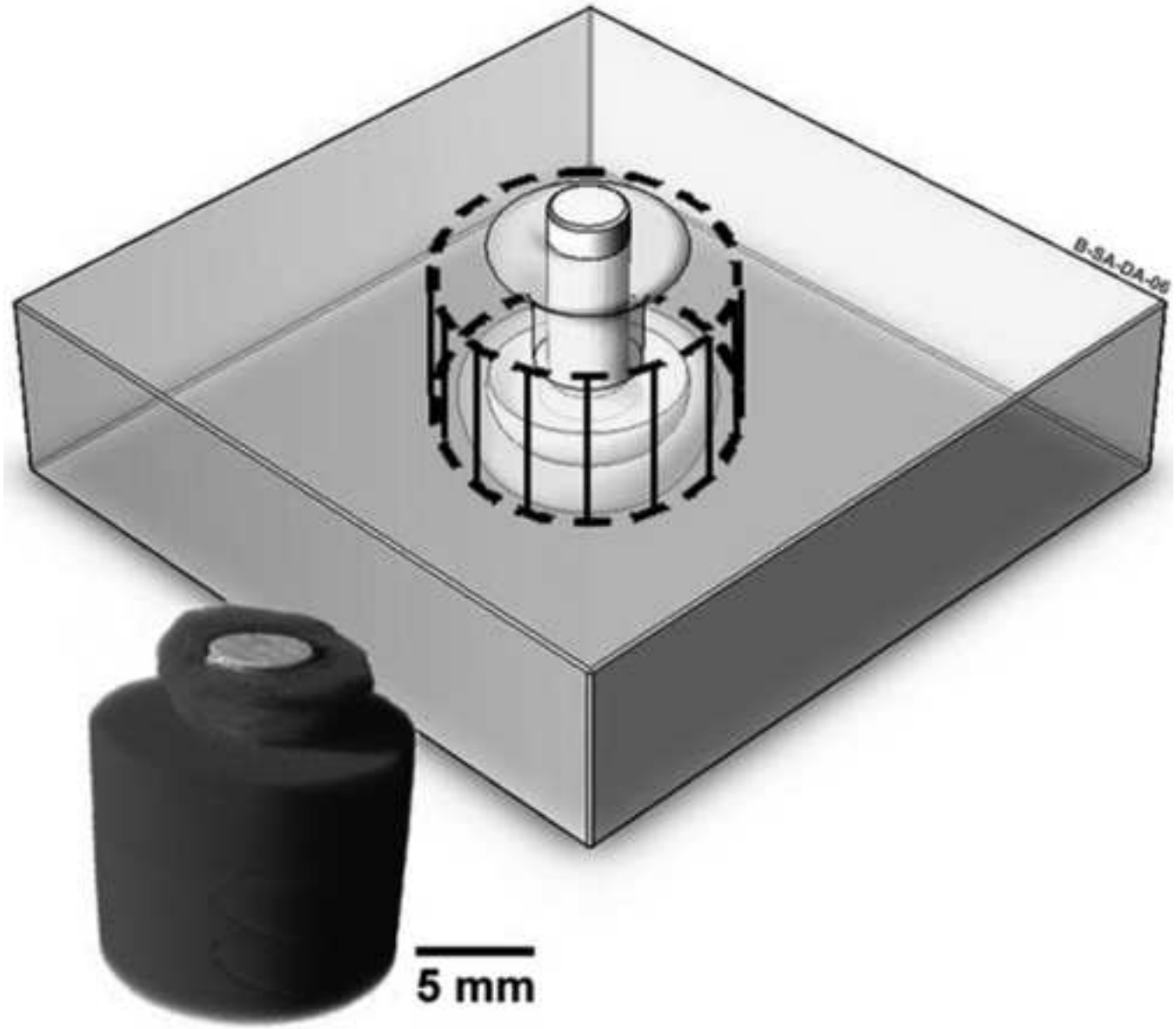

Figure 7

Click here to download high resolution image

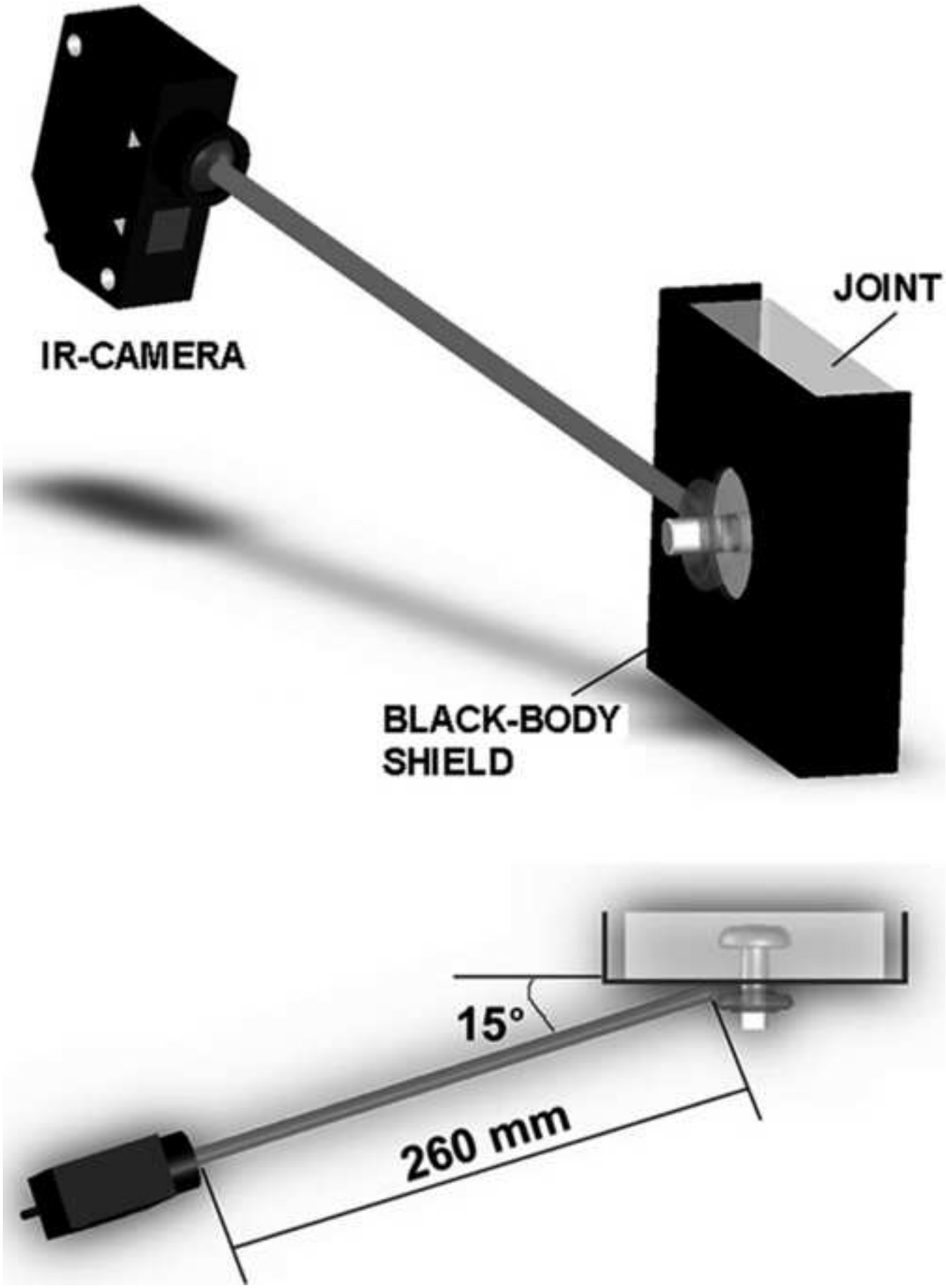

Figure 8

Click here to download high resolution image

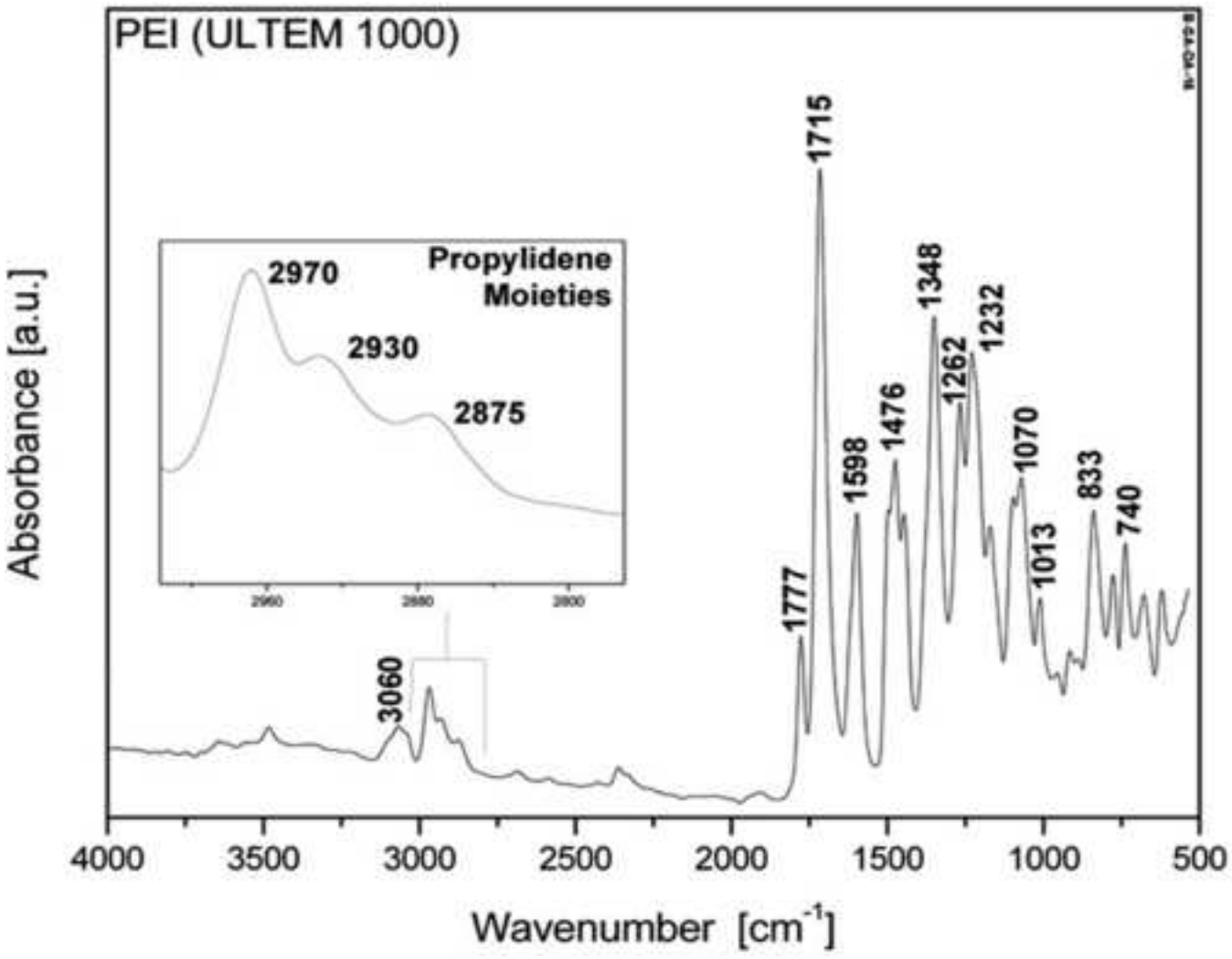

Figure 9

Click here to download high resolution image

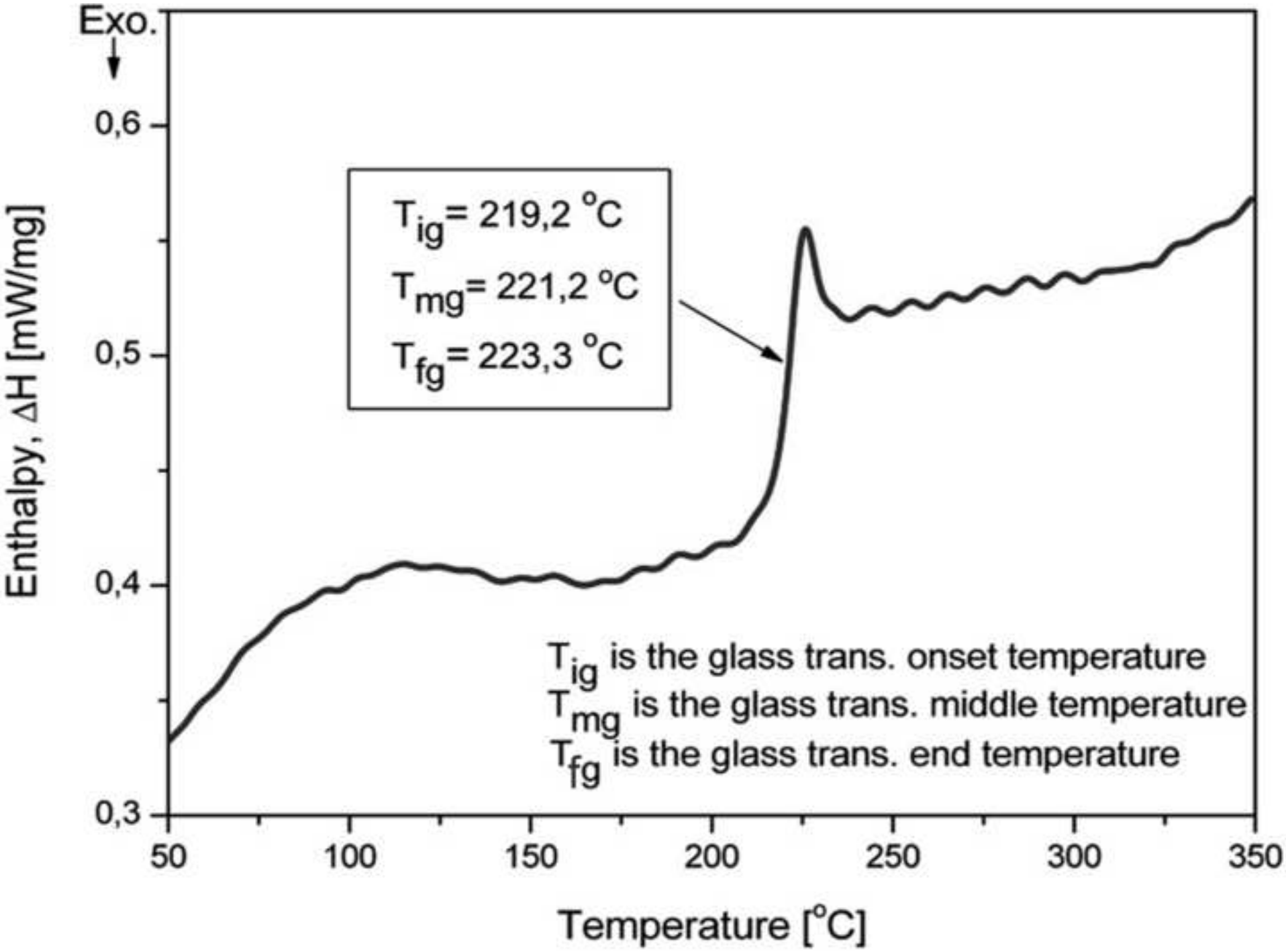

Figure 10

Click here to download high resolution image

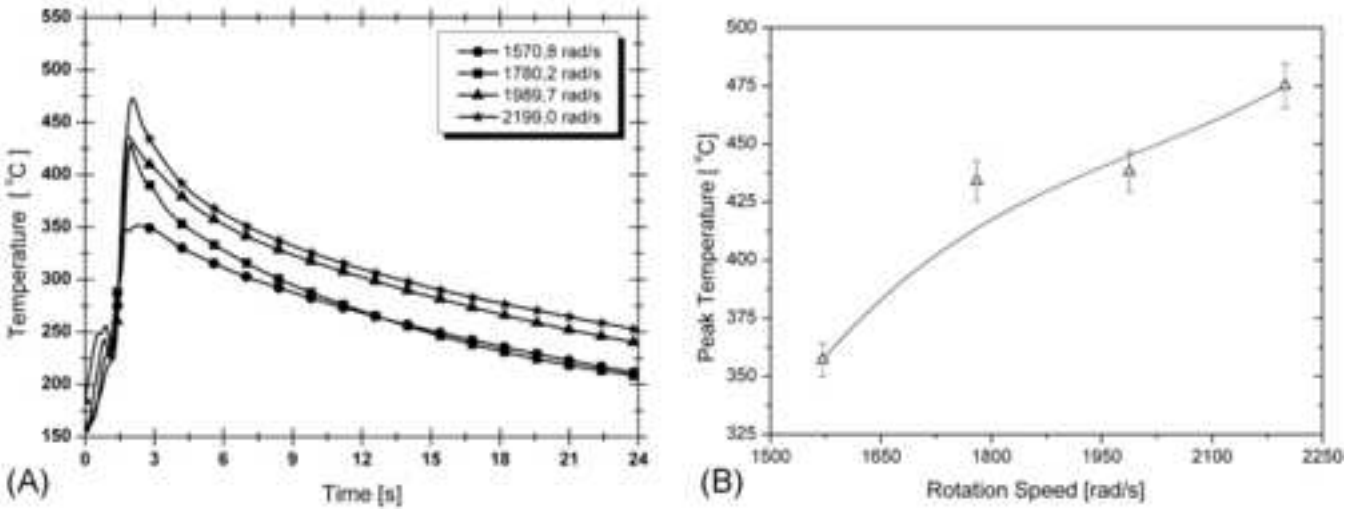

Figure 11

Click here to download high resolution image

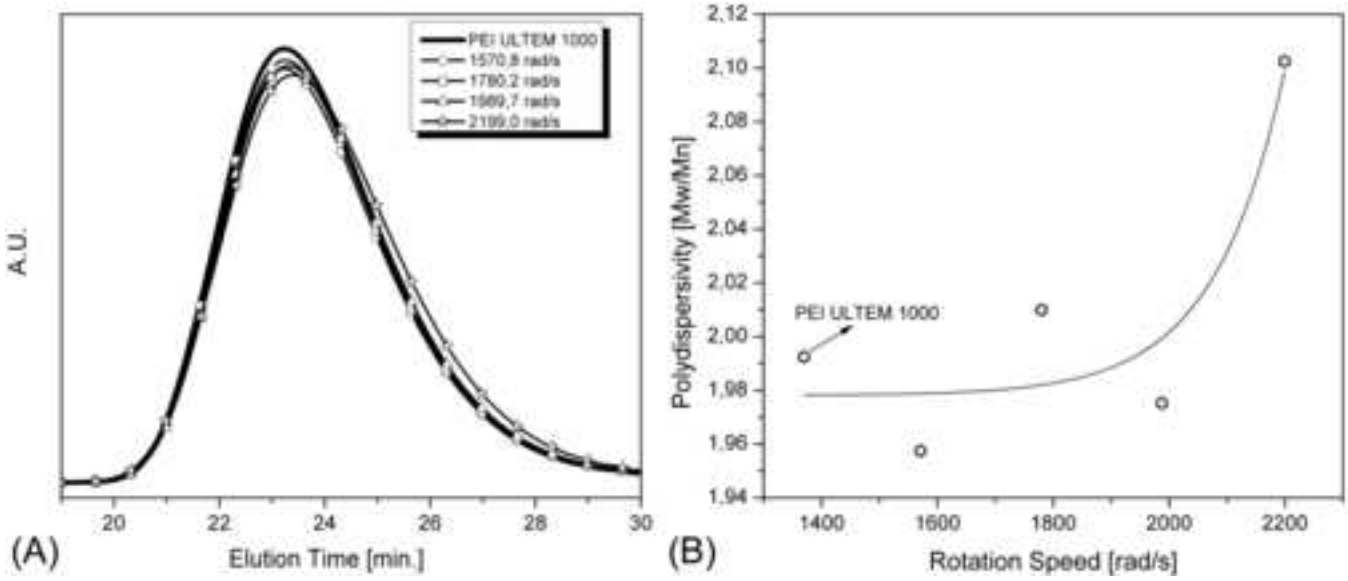

Figure 12

Click here to download high resolution image

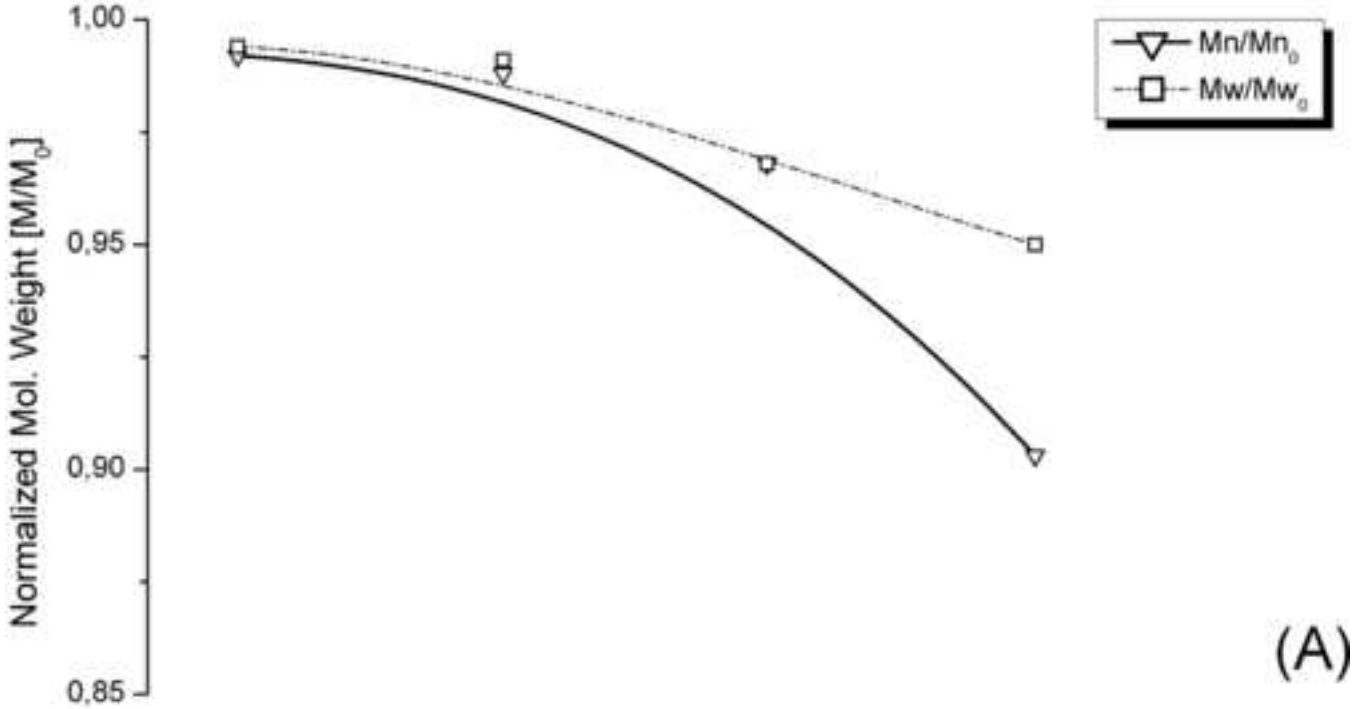

(A)

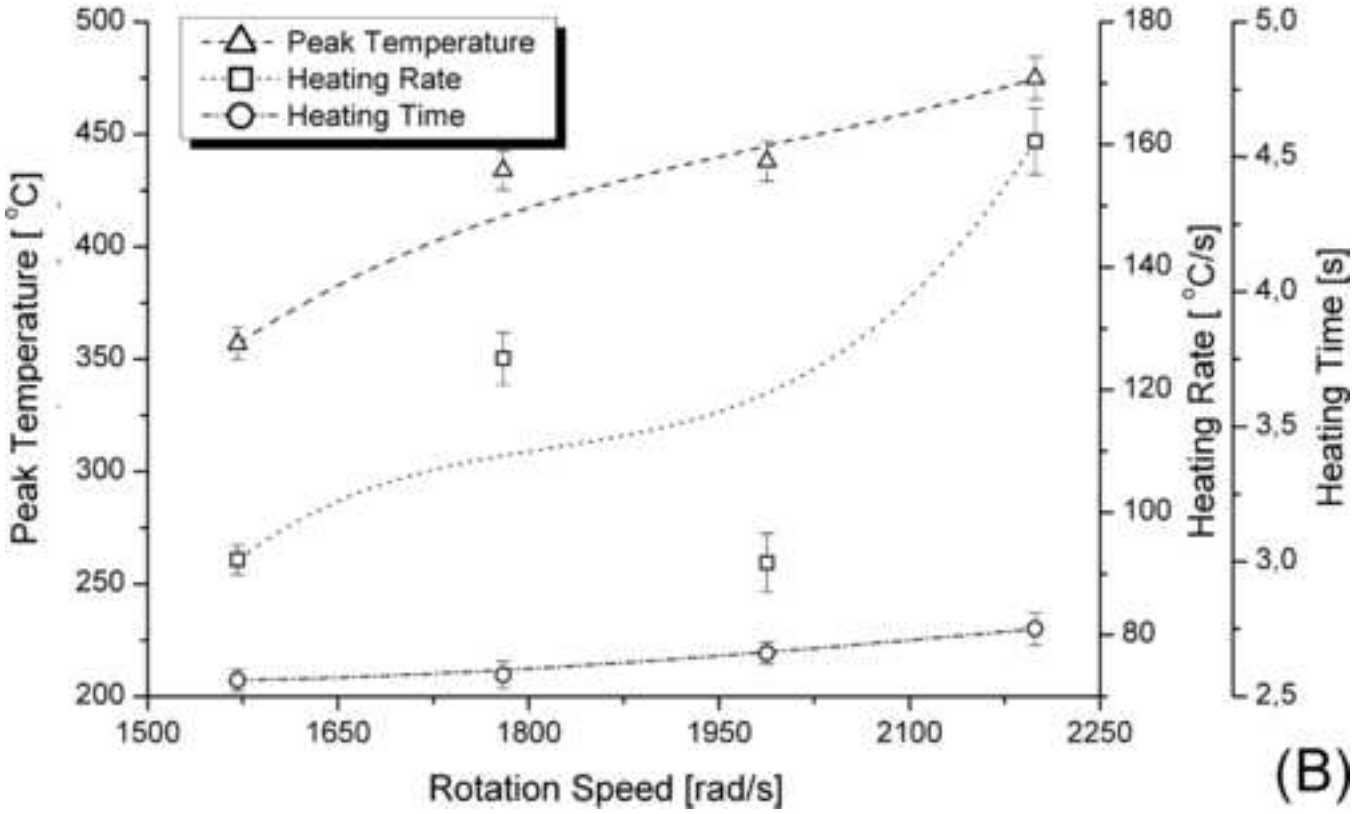

(B)

Figure 13

Click here to download high resolution image

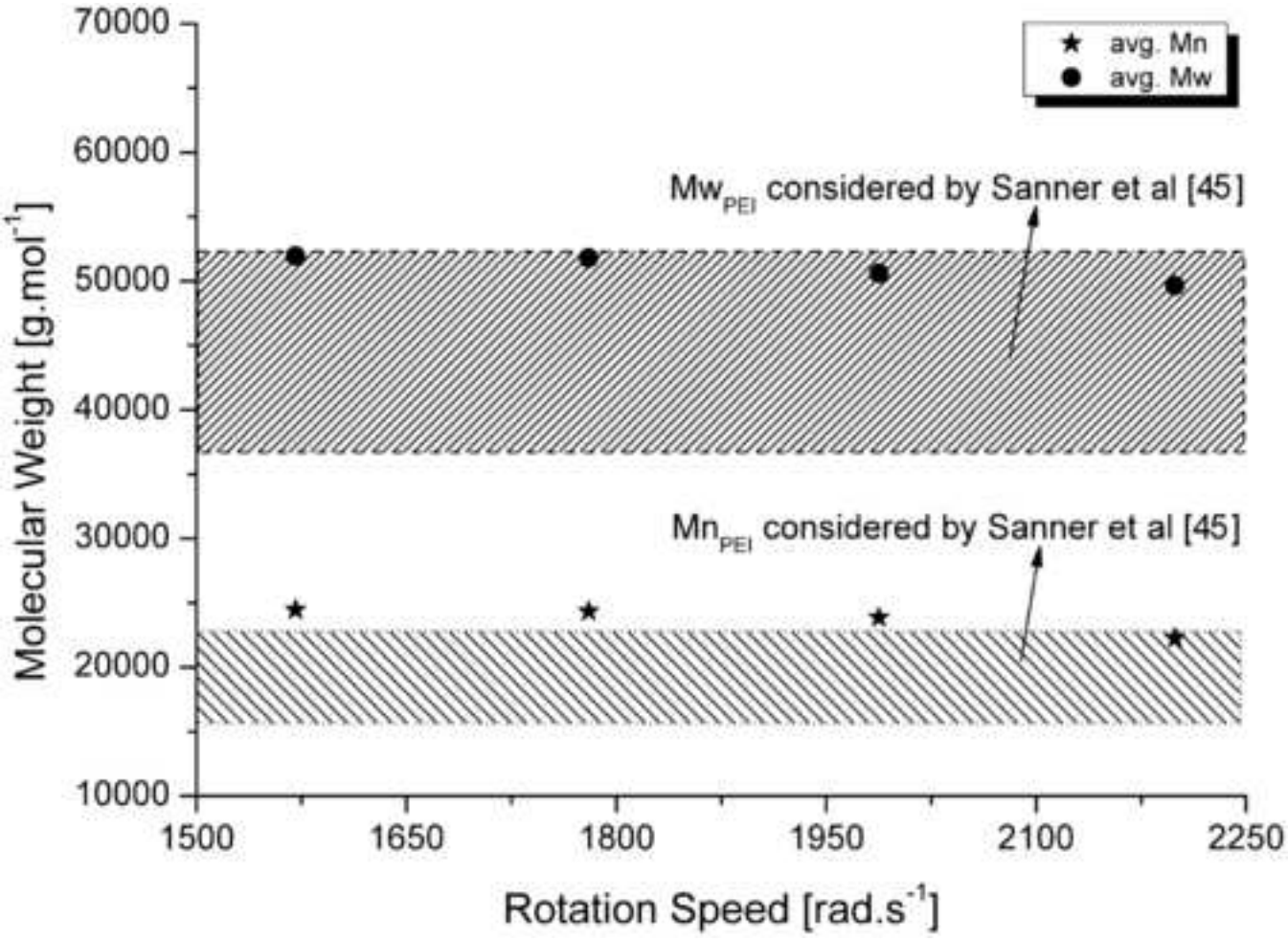

Figure 14

Click here to download high resolution image

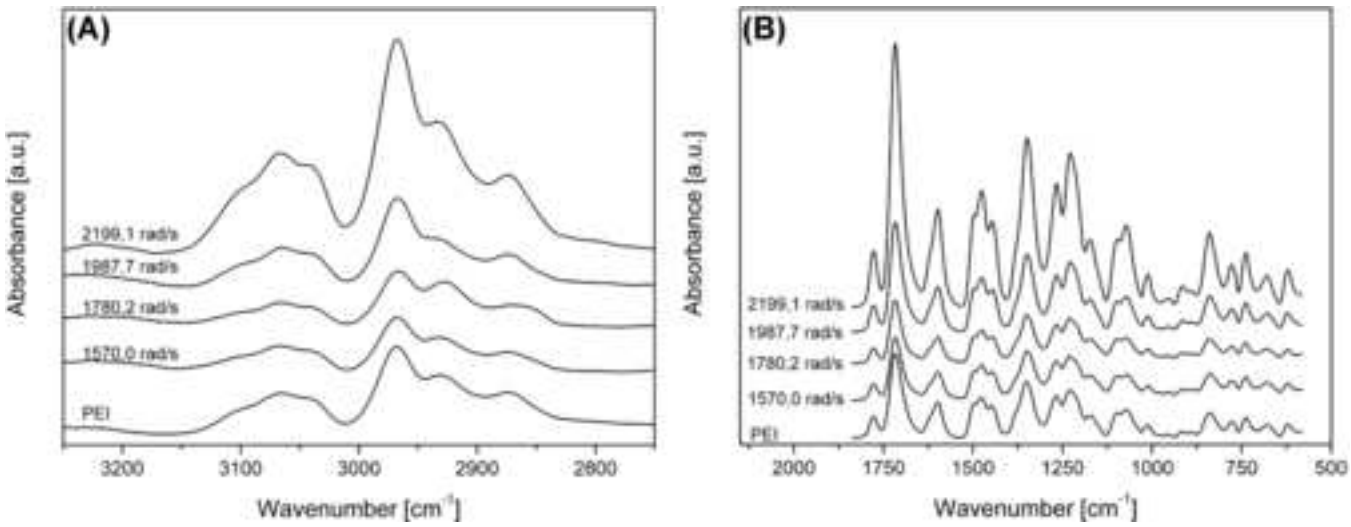

Figure 15

Click here to download high resolution image

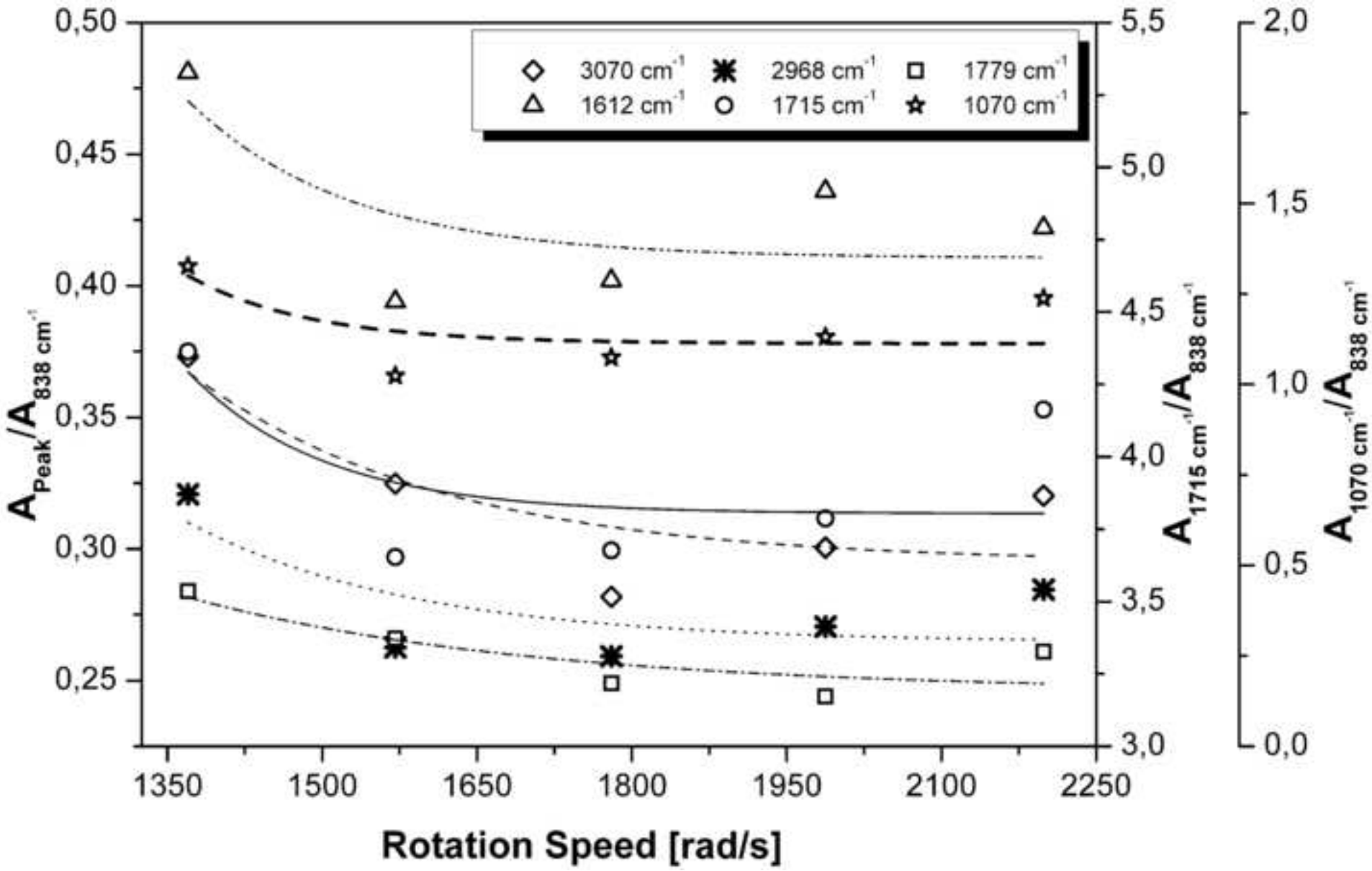

Figure 16

Click here to download high resolution image

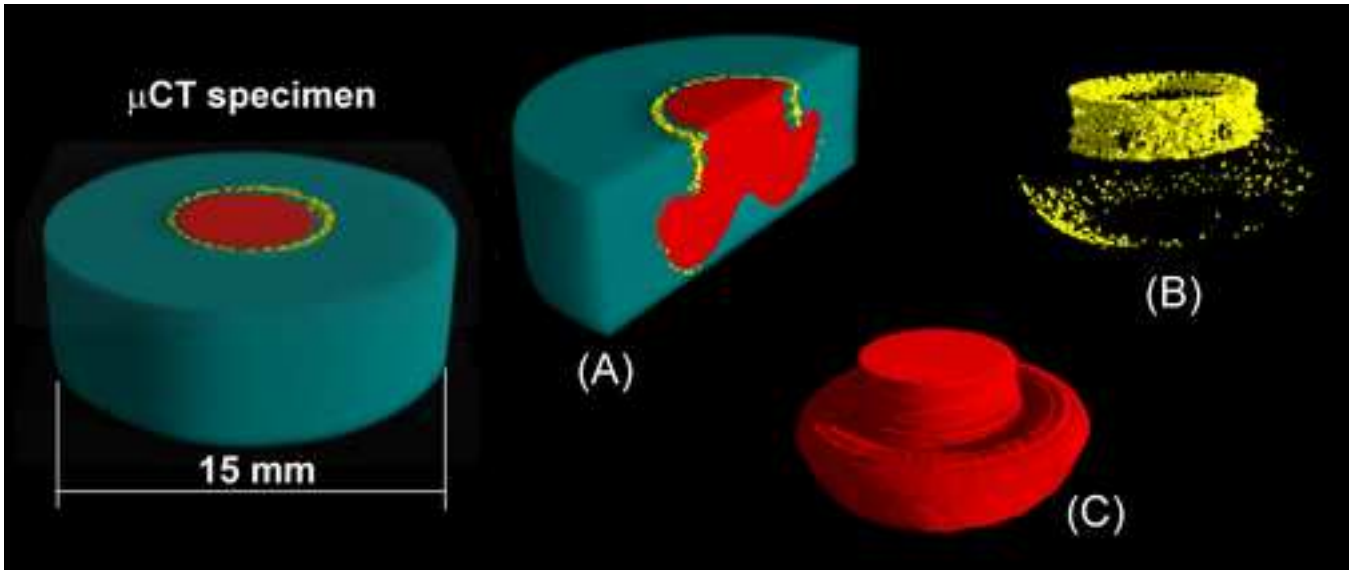

Figure 17
Click here to download high resolution image